Supplement of Clim. Past, 13, 1213–1226, 2017
https://doi.org/10.5194/cp-13-1213-2017-supplement

Climate of the Past
Open Access
EGU

Supplement of

Sources and characteristics of terrestrial carbon in Holocene-scale sediments of the East Siberian Sea

Kirsi Keskitalo et al.

Correspondence to: Örjan Gustafsson (orjan.gustafsson@aces.su.se)

Supplementary information

Tables and figures

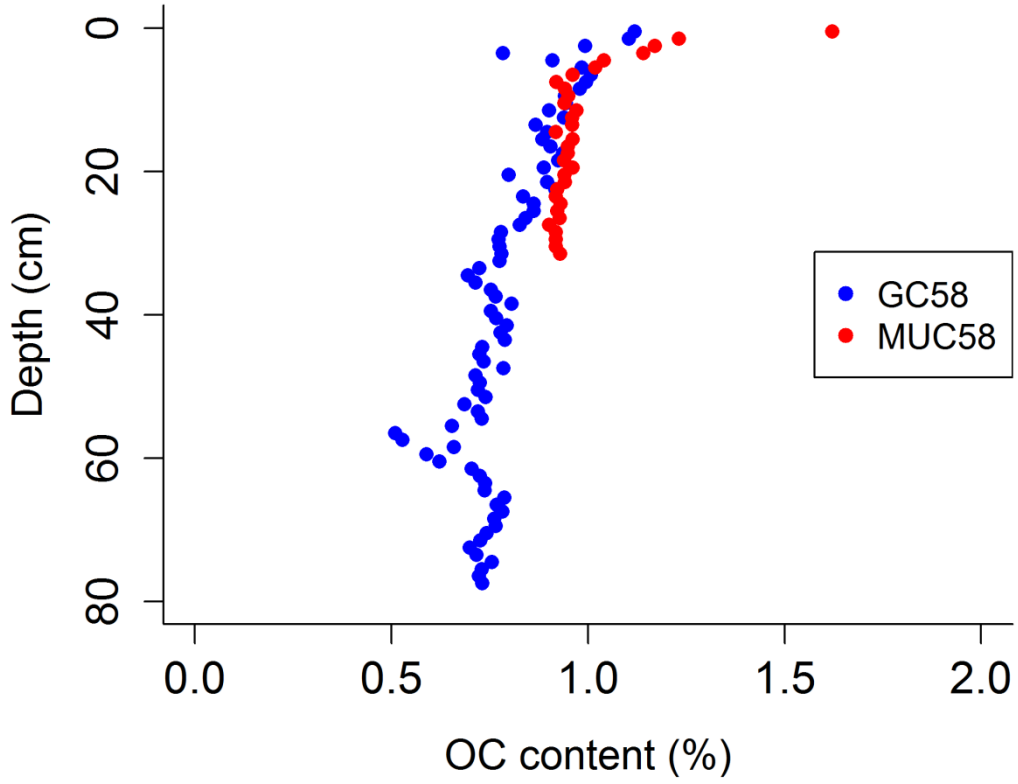

Figure S1. Comparison between the organic carbon (OC) content (%) of the sediment cores GC58 and MUC58. Based on the comparison, we deduced that the top 3cm of GC58 were lost during sampling.

Table S1. Total organic carbon (TOC) content, stable carbon isotopes ($\delta^{13}C$) and calibrated radiocarbon isotopes of bulk carbon (cal $\Delta^{14}C$) in the sediment core GC58 that were used for source apportionment calculations.

Corrected depth* (cm)	TOC (%)	$\delta^{13}C$ (‰)	Cal $\Delta^{14}C$ (‰)
3.5	1.12	-23.23	-400.17
4.5	1.10	-23.07	
5.5	0.99	-23.25	
6.5	0.78	-23.10	
7.5	0.91	-23.16	
8.5	0.99	-23.32	
9.5	1.01	-23.12	
10.5	1.00	-23.42	
11.5	0.98	-23.48	
12.5	0.94	-23.39	
13.5	0.94	-23.19	-568.02
14.5	0.90	-23.32	
15.5	0.94	-23.38	
16.5	0.87	-23.49	
17.5	0.90	-23.61	
18.5	0.88	-23.56	
19.5	0.91	-23.61	
20.5	0.94	-23.44	
21.5	0.93	-23.62	
22.5	0.89	-23.57	
23.5	0.80	-23.50	-604.39
24.5	0.90	-23.56	
25.5	0.92	-23.59	
26.5	0.84	-23.76	
27.5	0.86	-23.57	
28.5	0.86	-23.88	
29.5	0.84	-23.61	
30.5	0.83	-24.33	
31.5	0.78	-24.08	
32.5	0.77	-24.22	
33.5	0.78	-23.89	-679.07
34.5	0.78	-24.14	
35.5	0.78	-24.24	
36.5	0.72	-24.73	
37.5	0.70	-24.54	
38.5	0.71	-24.63	-747.85
39.5	0.75	-24.37	
40.5	0.77	-24.82	
41.5	0.81	-24.75	
42.5	0.75	-24.95	
43.5	0.77	-25.07	-586.93
44.5	0.79	-24.91	

45.5	0.78	-24.91	
46.5	0.79	-24.93	
47.5	0.73	-24.86	-607.58
48.5	0.72	-24.93	
49.5	0.74	-25.01	
50.5	0.79	-24.85	
51.5	0.71	-25.08	
52.5	0.73	-25.05	
53.5	0.72	-25.11	-680.66
54.5	0.74	-24.85	
55.5	0.69	-25.34	
56.5	0.72	-25.44	
57.5	0.73	-25.51	
58.5	0.65	-25.66	
59.5	0.51	-25.65	
60.5	0.53	-25.68	
61.5	0.66	-25.55	
62.5	0.59	-25.65	
63.5	0.62	-25.74	-771.72
64.5	0.71	-25.59	
65.5	0.73	-25.68	
66.5	0.74	-25.66	
67.5	0.74	-25.66	
68.5	0.79	-25.53	
69.5	0.77	-25.51	
70.5	0.78	-25.63	
71.5	0.76	-25.60	
72.5	0.77	-25.59	
73.5	0.74	-25.66	-764.43
74.5	0.73	-25.60	
75.5	0.70	-25.59	
76.5	0.72	-25.70	
77.5	0.76	-25.65	
78.5	0.73	-25.84	
79.5	0.72	-25.75	
80.5	0.73	-25.58	

*Corrected depth is the original depth + 3 cm to account for core top loss during sampling (Sect. 2.4).

Table S2. The amount of excess ^{210}Pb (Bq g^{-1}) and natural logarithm (ln) of excess^{210}Pb in the sediment core MUC58 and age chronology (CRC and CIC models) presented as age (yr) and resulting year of deposition. The CRC model assumes a constant rate of supply of ^{210}Pb fallout, as the CIC assumes the initial concentration of ^{210}Pb to be constant (Appleby & Oldfield, 1978). The highest ^{137}Cs peak was in 4.5 cm depth.

Depth (cm)	Excess ^{210}Pb (Bq g^{-1})	Ln of excess ^{210}Pb	Age (yr) with CRC model	Resulting year with CRC model	Age (yr) with CIC model	Resulting year with CIC model	OC flux (g m^{-2} yr^{-1})
0.5	0.062	-2.78	0	2014	4	2010	6.1
1.5	0.061	-2.79	6	2008	12	2002	4.6
2.5	0.054	-2.92	14	2000	20	1994	4.4
3.5	0.049	-3.02	23	1991	28	1986	4.3
4.5	0.024	-3.73	35	1979	36	1978	3.9
5.5	0.016	-4.11	42	1972	44	1970	3.8
6.5	0.014	-4.24	49	1965	52	1962	3.6
7.5	0.021	-3.86	55	1959	60	1954	3.4
8.5	0.016	-4.145	69	1945	68	1946	3.5
9.5	0.006	-5.16	85	1929	75	1939	3.6
10.5	0.001	-6.67	94	1920	83	1931	3.5
11.5	0.012	-4.41	96	1918	91	1923	3.6
12.5	0.005	-5.25	134	1880	99	1915	0.4

Table S3. Biomarker data for the sediment core GC58. S = syringyl phenols, V = vanillyl phenols, C = cinnamyl phenols, 3,5-Bd = 3,5-Dihydroxybenzoic acid, Cut = sum of all cutin acids, FA = sum of all CuO-oxidation-derived fatty acids, Lig = sum of all lignin phenols, Sd = syringic acid, Sl = syringaldehyde, Vd = vanillic acid, Vl = vanillin (see Supplementary Table S4 for full list of compounds and their origin).

Corrected depth*	S	V	C	3,5-Bd	Cut	FA	Lig	S/V	C/V	Sd/Sl	Vd/Vl	3,5-Bd/V
cm	mg g OC $^{-1}$	mg g OC $^{-1}$	mg g OC $^{-1}$	mg g OC $^{-1}$	mg g OC $^{-1}$	mg g OC $^{-1}$	mg g OC $^{-1}$					
3.5	0.05	0.13	0.04	0.1225	0.27	5.35	0.2244	0.42	0.31	0.59	0.95	0.94
4.5	0.08	0.12	0.07	0.0898	0.30	3.17	0.2700	0.66	0.60	0.64	0.95	0.75
5.5	0.07	0.08	0.03	0.1148	0.24	2.55	0.1770	0.90	0.37	0.59	0.00	1.47
6.5	0.07	0.12	0.03	0.1008	0.30	2.55	0.2318	0.59	0.26	0.63	0.78	0.81
7.5	0.07	0.12	0.03	0.1486	0.30	2.06	0.2222	0.59	0.23	0.52	0.88	1.22
8.5	0.05	0.12	0.03	0.1055	0.27	1.38	0.2017	0.39	0.24	0.66	1.55	0.85
9.5	0.04	0.13	0.04	0.0696	0.27	1.26	0.2071	0.28	0.28	0.69	2.10	0.52
10.5	0.05	0.14	0.04	0.1043	0.28	1.41	0.2349	0.37	0.31	0.74	1.66	0.75
11.5	0.10	0.21	0.09	0.1083	0.34	1.31	0.4051	0.49	0.43	0.59	1.12	0.51
12.5	0.05	0.15	0.03	0.0978	0.34	1.53	0.2304	0.33	0.22	0.75	1.17	0.66
13.5	0.04	0.09	0.03	0.0866	0.29	1.35	0.1603	0.43	0.32	0.64	1.92	0.95
14.5	0.05	0.14	0.05	0.1276	0.35	1.43	0.2386	0.39	0.33	0.75	1.30	0.92
15.5	0.05	0.10	0.03	0.0917	0.27	1.12	0.1763	0.48	0.35	0.66	1.35	0.95
16.5	0.05	0.16	0.03	0.1005	0.28	1.40	0.2383	0.33	0.19	0.60	1.32	0.64
17.5	0.05	0.14	0.05	0.1092	0.35	1.43	0.2356	0.39	0.34	0.78	1.59	0.80
18.5	0.05	0.12	0.04	0.0741	0.33	1.32	0.2125	0.45	0.38	0.64	1.35	0.64
19.5	0.05	0.13	0.04	0.0831	0.30	1.14	0.2190	0.38	0.29	0.71	1.46	0.63
20.5	0.05	0.09	0.02	0.0969	0.30	1.20	0.1668	0.52	0.25	0.77	1.93	1.03
21.5	0.05	0.10	0.05	0.0928	0.34	1.28	0.2033	0.50	0.46	0.76	1.78	0.90
22.5	0.06	0.16	0.05	0.1101	0.37	1.56	0.2716	0.40	0.29	0.72	1.41	0.69
23.5	0.07	0.17	0.05	0.1140	0.38	1.76	0.2973	0.41	0.29	0.76	1.62	0.65
24.5	0.06	0.15	0.05	0.0931	0.33	1.19	0.2595	0.38	0.30	0.80	2.10	0.60
25.5	0.06	0.15	0.04	0.0830	0.37	1.16	0.2581	0.41	0.26	0.73	2.45	0.54
26.7	0.07	0.15	0.05	0.1321	0.41	1.31	0.2686	0.49	0.33	0.78	1.66	0.90
27.5	0.06	0.15	0.05	0.0829	0.31	0.95	0.2650	0.41	0.32	0.79	1.81	0.54

28.5	0.08	0.18	0.05	0.0812	0.16	1.01	0.3152	0.46	0.27	0.63	1.07	0.44
29.5	0.08	0.19	0.06	0.1247	0.40	1.28	0.3308	0.41	0.29	0.85	1.87	0.64
30.5	0.12	0.26	0.09	0.1479	0.52	1.22	0.4713	0.46	0.34	0.82	1.67	0.56
31.5	0.14	0.29	0.11	0.0942	0.60	1.31	0.5506	0.50	0.39	0.70	1.46	0.32
32.5	0.15	0.31	0.13	0.1060	0.55	1.19	0.5871	0.51	0.41	0.70	1.60	0.35
33.5	0.15	0.33	0.13	0.1388	0.54	1.29	0.6118	0.45	0.41	0.79	1.55	0.42
34.5	0.16	0.35	0.10	0.1264	0.57	1.44	0.6116	0.44	0.28	0.71	1.35	0.36
35.5	0.23	0.46	0.13	0.1608	0.70	1.49	0.8146	0.49	0.29	0.67	1.24	0.35
36.5	0.22	0.44	0.09	0.1100	0.49	0.90	0.7432	0.50	0.20	0.75	1.46	0.25
37.5	0.21	0.39	0.09	0.0997	0.66	0.79	0.6890	0.53	0.23	0.70	1.51	0.25
38.5	0.28	0.55	0.17	0.1922	0.82	1.28	1.0034	0.50	0.32	0.73	1.45	0.35
39.5	0.25	0.33	0.16	0.2636	0.91	1.27	0.7434	0.77	0.49	0.70	0.00	0.80
40.5	0.25	0.48	0.17	0.1434	0.71	1.20	0.8986	0.51	0.35	0.70	1.58	0.30
41.5	0.24	0.47	0.18	0.1524	0.82	0.97	0.8947	0.50	0.39	0.70	1.59	0.32
42.5	0.28	0.53	0.17	0.1501	0.87	0.95	0.9828	0.52	0.32	0.70	1.46	0.28
43.5	0.27	0.55	0.23	0.1655	0.90	1.04	1.0439	0.49	0.42	0.80	1.62	0.30
44.5	0.24	0.59	0.15	0.1357	0.52	0.83	0.9758	0.40	0.24	0.68	1.22	0.23
45.5	0.31	0.57	0.21	0.1540	1.02	1.00	1.0923	0.53	0.37	0.72	1.33	0.27
46.5	0.28	0.61	0.17	0.2329	0.86	1.17	1.0583	0.46	0.27	0.75	1.45	0.38
47.5	0.28	0.60	0.20	0.1796	0.89	1.07	1.0789	0.46	0.34	0.79	1.54	0.30
48.5	0.33	0.63	0.24	0.1880	1.03	1.11	1.1976	0.52	0.38	0.70	1.63	0.30
49.5	0.26	0.53	0.16	0.1326	0.84	0.87	0.9443	0.49	0.31	0.69	1.36	0.25
50.5	0.27	0.53	0.17	0.1713	0.81	0.91	0.9745	0.51	0.33	0.79	1.61	0.32
51.5	0.33	0.68	0.20	0.1953	0.95	1.32	1.2145	0.49	0.30	0.76	1.34	0.29
52.5	0.40	0.71	0.18	0.2140	0.94	1.05	1.2953	0.57	0.25	0.69	1.39	0.30
53.5	0.29	0.60	0.24	0.1764	0.92	0.93	1.1337	0.49	0.40	0.82	1.56	0.29
54.5	0.31	0.60	0.15	0.1932	0.97	1.01	1.0656	0.51	0.25	0.76	1.75	0.32
55.5	0.53	0.99	0.32	0.2323	1.15	0.96	1.8391	0.53	0.33	0.67	1.34	0.24
56.5	0.61	1.27	0.36	0.1990	0.72	0.88	2.2406	0.48	0.29	0.57	1.19	0.16
57.5	1.10	2.16	0.93	0.2084	1.58	0.86	4.1854	0.51	0.43	0.58	1.03	0.10
58.5	1.23	2.14	0.79	0.2092	1.69	0.87	4.1617	0.57	0.37	0.55	1.09	0.10
59.5	1.21	2.33	0.93	0.1797	1.18	1.38	4.4684	0.52	0.40	0.57	1.07	0.08

60.5	1.23	2.18	1.02	0.2039	1.73	1.04	4.4373	0.57	0.47	0.58	1.14	0.09
61.5	1.35	2.77	0.79	0.2295	1.64	1.04	4.9075	0.49	0.28	0.61	1.05	0.08
62.5	1.51	2.74	1.18	0.2587	1.90	1.27	5.4277	0.55	0.43	0.53	0.95	0.09
63.5	1.80	3.20	1.22	0.2237	1.74	0.97	6.2276	0.56	0.38	0.47	0.85	0.07
64.5	1.27	2.40	0.93	0.2790	1.81	1.26	4.6095	0.53	0.39	0.53	0.96	0.12
65.5	1.15	2.07	0.94	0.2470	1.79	0.92	4.1586	0.55	0.45	0.56	1.07	0.12
66.5	1.27	2.38	0.74	0.2618	1.79	1.02	4.3928	0.53	0.31	0.54	1.07	0.11
67.5	1.00	1.79	0.85	0.1983	1.57	0.71	3.6389	0.56	0.48	0.61	1.21	0.11
68.5	1.19	2.18	0.84	0.2506	1.76	0.91	4.1993	0.55	0.38	0.52	0.98	0.12
69.5	0.85	1.71	0.53	0.1673	0.84	0.68	3.0966	0.50	0.31	0.61	1.18	0.10
70.5	1.31	2.46	0.92	0.3261	1.78	0.97	4.7013	0.53	0.38	0.54	1.01	0.13
71.5	1.25	2.32	1.02	0.2840	1.73	1.01	4.5828	0.54	0.44	0.58	1.09	0.12
72.5	1.20	2.19	0.96	0.2213	1.81	0.93	4.3449	0.55	0.44	0.58	1.14	0.10
73.5	1.04	2.07	0.72	0.2024	1.13	0.80	3.8276	0.50	0.35	0.55	1.03	0.10
74.5	1.41	2.68	1.22	0.2547	1.97	1.01	5.3135	0.53	0.45	0.50	0.87	0.09
75.5	1.39	2.62	1.16	0.3377	1.97	1.29	5.1729	0.53	0.44	0.61	1.08	0.13
76.5	1.30	2.48	1.09	0.2550	1.93	1.23	4.8662	0.52	0.44	0.53	0.95	0.10
77.5	1.14	2.00	1.07	0.2116	1.66	0.93	4.2050	0.57	0.53	0.54	1.06	0.11
78.5	1.25	2.30	1.02	0.2549	1.81	1.06	4.5619	0.54	0.44	0.53	1.00	0.11
79.5	1.23	2.15	1.02	0.2753	1.94	1.26	4.4096	0.57	0.48	0.55	1.17	0.13
80.5	1.22	2.22	1.09	0.2613	1.99	1.02	4.5331	0.55	0.49	0.56	1.11	0.12

* Corrected depth is the original depth + 3 cm to account for core top loss during sampling (Sect. 2.4)

Table S4. CuO-derived compounds (adapted from Tesi et al. 2014 and references therein). MS means that the compound has multiple sources but is relatively abundant in the source mentioned.

Group name	Name	Abbreviation	Source
Lignin phenols	Vanillyl phenols	V	Cell walls of angiosperm/gymnosperm vascular plants
	Vanillin	Vl	
	Acetovanillone	Vn	
	Vanillic acid	Vd	
	Syringyl phenols	S	Cell walls of angiosperm vascular plants
	Syringaldehyde	Sl	
	Acetosyringone	Sn	
	Syringic acid	Sd	
	Cinnamyl phenols	C	
	p-Coumaric acid	pCd	Non-woody vascular plant tissues
	Ferulic acid	Fd	
Cutin products	Hydroxyhexadecanoic acid	ω-C16	Leaves; blades and needles of vascular plants
	Hexadecan-1,16-dioic acid	C16DA	
	18-Hydroxyoctadec-9-enoic acid	ω-C18:1	
	7 or 8-Dihydroxy C16 x, ω-dioic acids	x-OH, C16DA	
	8, 9 or 10-Dihydroxy C16 acids	x,ω-OH C16	
Hydroxy benzene products	Benzoic acid	Bd	Phytoplankton and soil (MS)
	m-Hydroxybenzoic acid	m-Bd	
	3,5-Dihydroxybenzoic acid	3,5-Bd	Abundant in soil
Fatty acids	Octanoic acid	C8FA	Phytoplankton (MS)
	Decanoic acid	C10FA	Bacteria
	Dodecanoic acid	C12FA	Bacteria (MS)
	Tetradecanoic acid	C14FA	Phytoplankton (MS)
	Hexadecanoic acids	C16FA:1, C16FA	Phytoplankton and soil (also bacteria for C16FA:1) (MS)
	Octadecanoic acids	C18FA:1, C18FA	Phytoplankton and soil (also bacteria for C18FA:1) (MS)

Table S5. Source apportionment data from the Monte Carlo mixing model based on carbon isotopes ($\Delta^{14}C$, $\delta^{13}C$) as fractions (mean and median, %) for the sediment core GC58, including 5th (q05) and 9th (q95) percentiles and standard deviation (sd). Topsoil-PF (topsoil permafrost) refers to thaw of the active-layer permafrost, ICD-PF (Ice Complex deposit permafrost) represents old Pleistocene material from coastal erosion and marine OC (organic carbon) to primary production of phytoplankton.

	ICD-PF					Topsoil-PF					Marine OC				
Corrected depth (cm)	**mean**	**median**	**sd**	**q05**	**q95**	**mean**	**median**	**sd**	**q05**	**q95**	**mean**	**median**	**sd**	**q05**	**q95**
3.5	0.407	0.406	0.050	0.328	0.489	0.230	0.210	0.120	0.066	0.450	0.363	0.377	0.094	0.196	0.498
4.5	0.422	0.421	0.048	0.347	0.503	0.212	0.194	0.111	0.062	0.416	0.366	0.377	0.088	0.207	0.492
5.5	0.437	0.435	0.047	0.363	0.516	0.196	0.179	0.103	0.057	0.386	0.367	0.377	0.083	0.217	0.487
6.5	0.451	0.449	0.046	0.379	0.529	0.181	0.165	0.095	0.053	0.358	0.368	0.378	0.079	0.225	0.481
7.5	0.464	0.462	0.046	0.394	0.542	0.167	0.152	0.089	0.049	0.334	0.369	0.377	0.075	0.233	0.477
8.5	0.476	0.474	0.046	0.407	0.555	0.155	0.141	0.084	0.045	0.312	0.369	0.376	0.071	0.240	0.472
9.5	0.499	0.497	0.045	0.431	0.578	0.133	0.120	0.074	0.038	0.273	0.368	0.374	0.065	0.251	0.462
10.5	0.519	0.517	0.045	0.452	0.597	0.116	0.104	0.067	0.031	0.241	0.365	0.370	0.059	0.258	0.453
11.5	0.536	0.534	0.045	0.470	0.615	0.101	0.090	0.061	0.025	0.216	0.362	0.366	0.055	0.264	0.444
12.5	0.552	0.550	0.045	0.487	0.630	0.090	0.078	0.057	0.021	0.195	0.358	0.362	0.052	0.267	0.436
13.5	0.597	0.595	0.044	0.534	0.674	0.060	0.050	0.045	0.010	0.142	0.342	0.346	0.045	0.265	0.412
14.5	0.625	0.623	0.045	0.561	0.702	0.046	0.036	0.040	0.006	0.115	0.329	0.331	0.044	0.255	0.397
15.5	0.642	0.641	0.046	0.575	0.719	0.038	0.029	0.037	0.004	0.101	0.319	0.321	0.044	0.246	0.388
16.5	0.651	0.650	0.047	0.583	0.728	0.035	0.026	0.035	0.003	0.094	0.314	0.315	0.044	0.241	0.384
17.5	0.654	0.653	0.047	0.586	0.732	0.034	0.025	0.035	0.003	0.092	0.312	0.313	0.044	0.238	0.382
18.5	0.653	0.652	0.047	0.587	0.731	0.035	0.025	0.035	0.003	0.093	0.312	0.314	0.044	0.238	0.381
19.5	0.650	0.648	0.046	0.586	0.728	0.037	0.027	0.036	0.003	0.098	0.313	0.315	0.044	0.239	0.381
20.5	0.645	0.643	0.046	0.583	0.724	0.040	0.030	0.037	0.004	0.105	0.314	0.317	0.044	0.239	0.382
21.5	0.641	0.638	0.046	0.579	0.720	0.044	0.034	0.039	0.005	0.114	0.314	0.317	0.044	0.239	0.382
22.5	0.639	0.635	0.045	0.578	0.718	0.049	0.039	0.041	0.005	0.123	0.312	0.315	0.044	0.236	0.380
23.5	0.638	0.634	0.045	0.577	0.717	0.054	0.044	0.043	0.006	0.131	0.308	0.311	0.044	0.232	0.376
24.5	0.639	0.635	0.045	0.578	0.719	0.059	0.049	0.044	0.008	0.140	0.302	0.305	0.044	0.226	0.370
25.5	0.641	0.637	0.045	0.581	0.722	0.064	0.055	0.046	0.010	0.148	0.294	0.297	0.044	0.218	0.362
26.5	0.646	0.641	0.045	0.585	0.727	0.070	0.061	0.047	0.011	0.156	0.285	0.287	0.044	0.209	0.353

27.5	0.651	0.647	0.045	0.591	0.733	0.075	0.067	0.048	0.014	0.163	0.274	0.275	0.044	0.198	0.343
28.5	0.658	0.654	0.045	0.598	0.740	0.081	0.073	0.049	0.016	0.170	0.261	0.263	0.044	0.185	0.331
29.5	0.667	0.662	0.045	0.607	0.750	0.086	0.079	0.049	0.017	0.177	0.247	0.249	0.045	0.170	0.318
30.5	0.676	0.670	0.045	0.618	0.760	0.091	0.084	0.050	0.019	0.183	0.233	0.235	0.045	0.155	0.304
31.5	0.687	0.680	0.046	0.629	0.772	0.095	0.089	0.051	0.021	0.190	0.218	0.220	0.046	0.139	0.291
32.5	0.699	0.691	0.046	0.642	0.786	0.099	0.093	0.052	0.021	0.196	0.202	0.205	0.047	0.122	0.277
33.5	0.711	0.703	0.047	0.654	0.800	0.102	0.096	0.054	0.021	0.200	0.187	0.190	0.049	0.104	0.264
34.5	0.724	0.716	0.047	0.668	0.817	0.103	0.097	0.055	0.020	0.205	0.172	0.175	0.050	0.087	0.251
35.5	0.738	0.729	0.048	0.681	0.833	0.104	0.098	0.057	0.017	0.209	0.158	0.161	0.051	0.070	0.239
36.5	0.753	0.743	0.049	0.695	0.849	0.103	0.097	0.059	0.015	0.211	0.144	0.147	0.052	0.055	0.227
37.5	0.767	0.756	0.049	0.709	0.865	0.102	0.095	0.060	0.012	0.211	0.131	0.134	0.053	0.041	0.217
38.5	0.781	0.770	0.050	0.722	0.879	0.099	0.092	0.061	0.009	0.213	0.120	0.121	0.054	0.030	0.207
39.5	0.794	0.784	0.054	0.728	0.894	0.098	0.089	0.066	0.006	0.218	0.109	0.109	0.054	0.021	0.200
40.5	0.606	0.633	0.141	0.328	0.789	0.141	0.091	0.146	0.011	0.448	0.253	0.253	0.076	0.132	0.376
41.5	0.638	0.644	0.092	0.477	0.774	0.123	0.097	0.096	0.024	0.315	0.239	0.240	0.063	0.137	0.341
42.5	0.654	0.652	0.066	0.552	0.762	0.116	0.102	0.068	0.032	0.248	0.230	0.231	0.057	0.137	0.322
43.5	0.662	0.658	0.060	0.574	0.759	0.112	0.104	0.060	0.030	0.225	0.226	0.226	0.054	0.137	0.313
44.5	0.666	0.664	0.061	0.576	0.766	0.108	0.101	0.059	0.025	0.218	0.225	0.225	0.053	0.139	0.312
45.5	0.671	0.669	0.061	0.580	0.772	0.101	0.093	0.058	0.021	0.211	0.227	0.227	0.052	0.144	0.313
46.5	0.679	0.676	0.060	0.590	0.778	0.092	0.083	0.055	0.017	0.196	0.229	0.229	0.051	0.149	0.313
47.5	0.690	0.686	0.060	0.602	0.788	0.081	0.072	0.051	0.014	0.179	0.229	0.228	0.050	0.151	0.311
48.5	0.699	0.695	0.060	0.610	0.797	0.075	0.066	0.049	0.012	0.169	0.227	0.226	0.049	0.150	0.308
49.5	0.709	0.706	0.060	0.621	0.809	0.068	0.059	0.047	0.011	0.159	0.222	0.221	0.048	0.146	0.302
50.5	0.722	0.719	0.061	0.633	0.824	0.062	0.053	0.045	0.009	0.150	0.215	0.214	0.048	0.140	0.294
51.5	0.738	0.734	0.061	0.649	0.840	0.057	0.047	0.043	0.008	0.139	0.205	0.205	0.048	0.130	0.283
52.5	0.753	0.749	0.062	0.664	0.855	0.052	0.042	0.041	0.006	0.132	0.195	0.194	0.047	0.121	0.272
53.5	0.769	0.765	0.062	0.679	0.872	0.048	0.038	0.039	0.005	0.125	0.183	0.182	0.047	0.109	0.259
54.5	0.786	0.783	0.063	0.696	0.887	0.044	0.034	0.038	0.004	0.118	0.170	0.169	0.047	0.096	0.246
55.5	0.819	0.817	0.064	0.725	0.918	0.038	0.028	0.036	0.003	0.107	0.143	0.142	0.046	0.071	0.219
56.5	0.848	0.850	0.065	0.749	0.944	0.034	0.023	0.037	0.002	0.104	0.118	0.116	0.045	0.048	0.194
57.5	0.871	0.876	0.066	0.768	0.962	0.032	0.019	0.040	0.001	0.105	0.097	0.094	0.044	0.032	0.173
58.5	0.888	0.896	0.067	0.782	0.976	0.031	0.017	0.042	0.001	0.105	0.081	0.076	0.042	0.020	0.155

59.5	0.900	0.909	0.067	0.792	0.983	0.031	0.016	0.044	0.001	0.107	0.070	0.064	0.041	0.013	0.142
60.5	0.906	0.915	0.066	0.798	0.988	0.032	0.017	0.044	0.000	0.111	0.063	0.057	0.040	0.009	0.133
61.5	0.906	0.912	0.065	0.801	0.991	0.034	0.021	0.043	0.000	0.112	0.060	0.055	0.040	0.006	0.131
62.5	0.897	0.899	0.064	0.797	0.992	0.041	0.030	0.042	0.000	0.119	0.062	0.057	0.042	0.004	0.136
63.5	0.870	0.863	0.073	0.768	0.992	0.061	0.052	0.052	0.000	0.159	0.069	0.065	0.047	0.003	0.152
64.5	0.718	0.832	0.281	0.075	0.981	0.180	0.072	0.235	0.002	0.738	0.102	0.076	0.092	0.010	0.294
65.5	0.751	0.844	0.244	0.177	0.979	0.155	0.065	0.206	0.003	0.642	0.095	0.076	0.076	0.013	0.247
66.5	0.765	0.842	0.222	0.253	0.980	0.142	0.065	0.188	0.002	0.575	0.093	0.078	0.071	0.012	0.230
67.5	0.778	0.840	0.200	0.336	0.982	0.129	0.063	0.167	0.002	0.500	0.093	0.080	0.067	0.010	0.219
68.5	0.794	0.841	0.175	0.427	0.983	0.113	0.061	0.144	0.002	0.415	0.093	0.082	0.063	0.010	0.207
69.5	0.811	0.843	0.147	0.518	0.982	0.097	0.057	0.119	0.002	0.334	0.092	0.084	0.059	0.010	0.194
70.5	0.827	0.845	0.120	0.608	0.980	0.083	0.054	0.093	0.002	0.260	0.090	0.085	0.054	0.011	0.184
71.5	0.840	0.846	0.097	0.679	0.980	0.073	0.054	0.071	0.002	0.201	0.087	0.083	0.050	0.011	0.173
72.5	0.851	0.847	0.080	0.730	0.980	0.066	0.055	0.055	0.002	0.168	0.083	0.081	0.047	0.011	0.163
73.5	0.856	0.848	0.074	0.756	0.982	0.064	0.055	0.050	0.002	0.159	0.079	0.077	0.045	0.010	0.156
74.5	0.857	0.854	0.081	0.730	0.984	0.068	0.056	0.058	0.002	0.176	0.076	0.072	0.045	0.009	0.153
75.5	0.851	0.862	0.101	0.673	0.986	0.076	0.055	0.078	0.002	0.221	0.073	0.067	0.047	0.007	0.155
76.5	0.840	0.867	0.128	0.590	0.988	0.088	0.055	0.103	0.001	0.283	0.071	0.064	0.050	0.006	0.161
77.5	0.826	0.869	0.158	0.501	0.990	0.102	0.056	0.130	0.001	0.361	0.072	0.061	0.055	0.005	0.173
78.5	0.809	0.869	0.187	0.402	0.992	0.117	0.057	0.154	0.001	0.442	0.074	0.060	0.061	0.005	0.189
79.5	0.779	0.861	0.229	0.253	0.992	0.139	0.059	0.187	0.001	0.561	0.083	0.064	0.074	0.004	0.229
80.5	0.724	0.836	0.282	0.090	0.995	0.171	0.067	0.225	0.000	0.687	0.105	0.079	0.101	0.002	0.313

* Corrected depth is the original depth + 3 cm to account for core top loss during sampling (Sect 2.4).

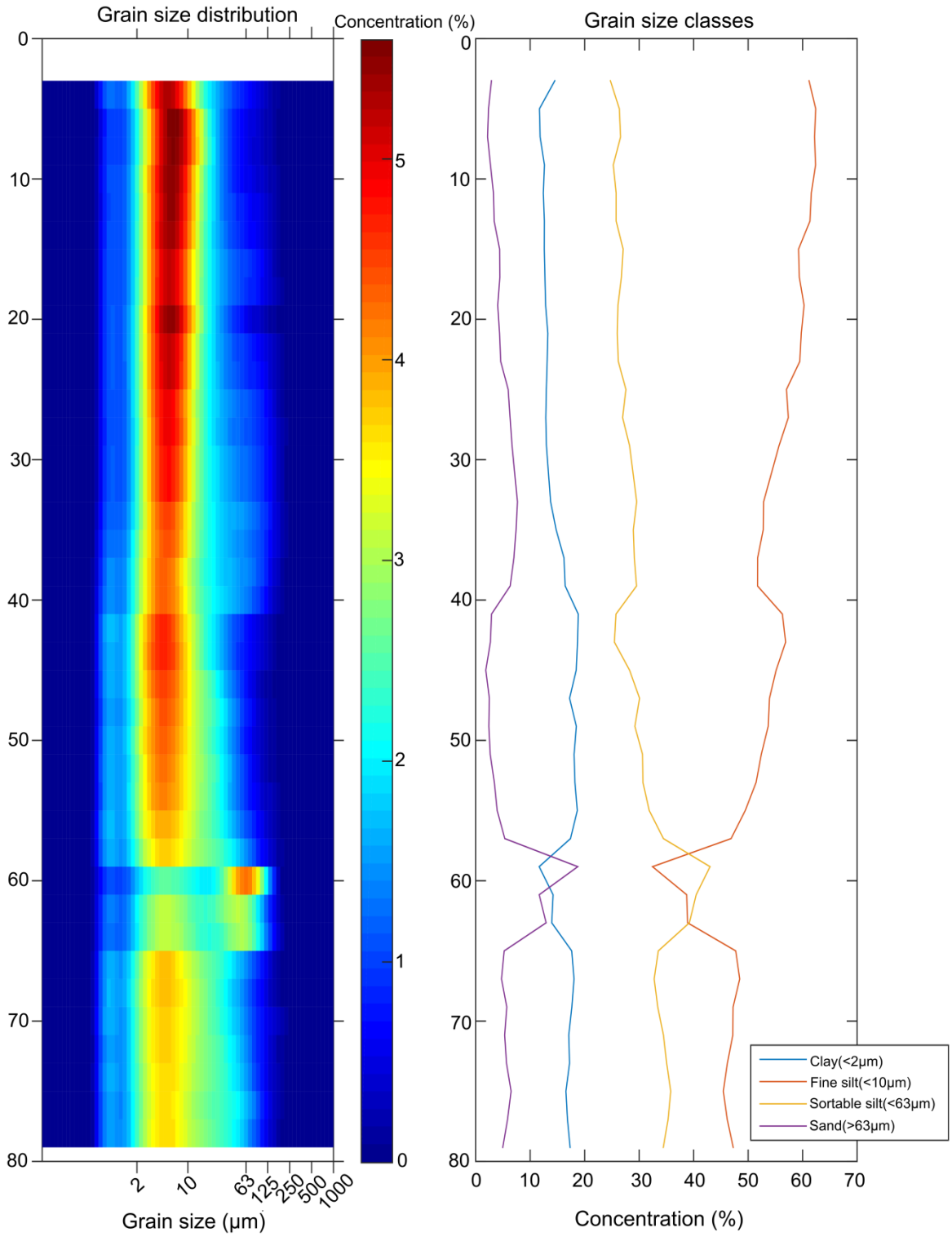

Figure S2. The grain size of the sediment core GC58. The GC58 core consists mainly of clay and silt with a fraction of sand around 60 cm of depth.

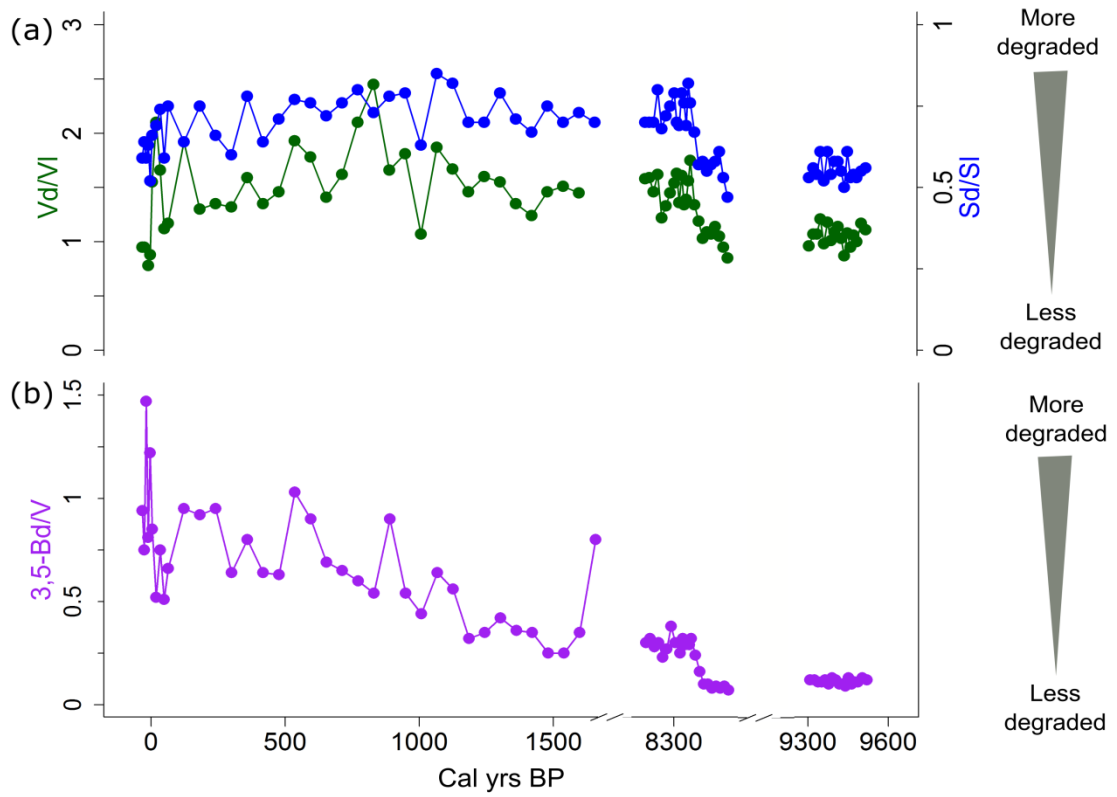

Figure S3. Degradation proxies for terrestrial organic carbon in the sediment core GC58. The x-axis has breaks due to gaps in the sediment chronology. (a) Syringyl acid to syringaldehyde (Sd/Sl) and vanillic acid to vanillin (Vd/Vl) ratios are a lignin-phenol based degradation proxy. The variability at the core top may also reflect the analytical uncertainty caused by very low lignin concentrations. (b) Also the ratio of 3,5-dihydrobenzoic acid to vanillyl phenols (3,5-Bd/V) provides information on degradation of terrestrial organic carbon. Higher values imply more degraded material for all the ratios as illustrated with the grey triangles. The 3,5-Bd/V values suggest a gradual increase in degradation from the bottom of the core to the top.

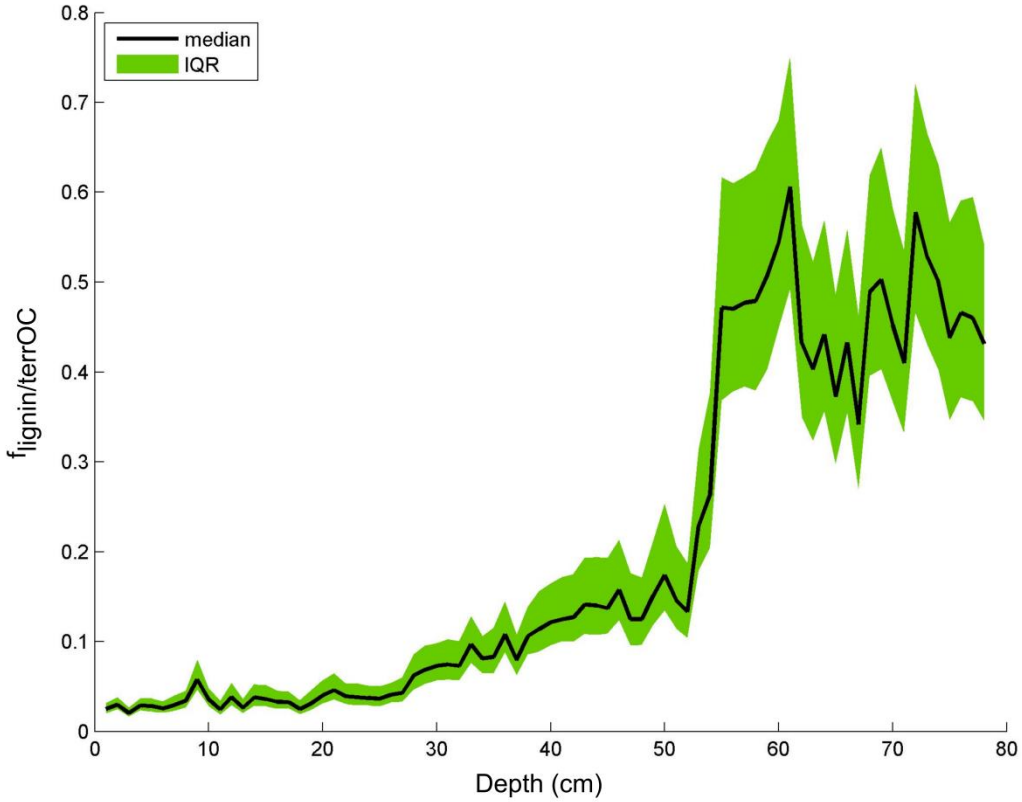

Figure S4. The ratio between the observed and expected lignin and terrestrial organic carbon (terrOC) ratios ($f_{lig/terrOC}$) with the interquartile range (IQR) for the sediment core GC58. The expected lignin values i.e. non-degraded lignin are taken from Tesi et al., (2016). See Supplementary methods for details.

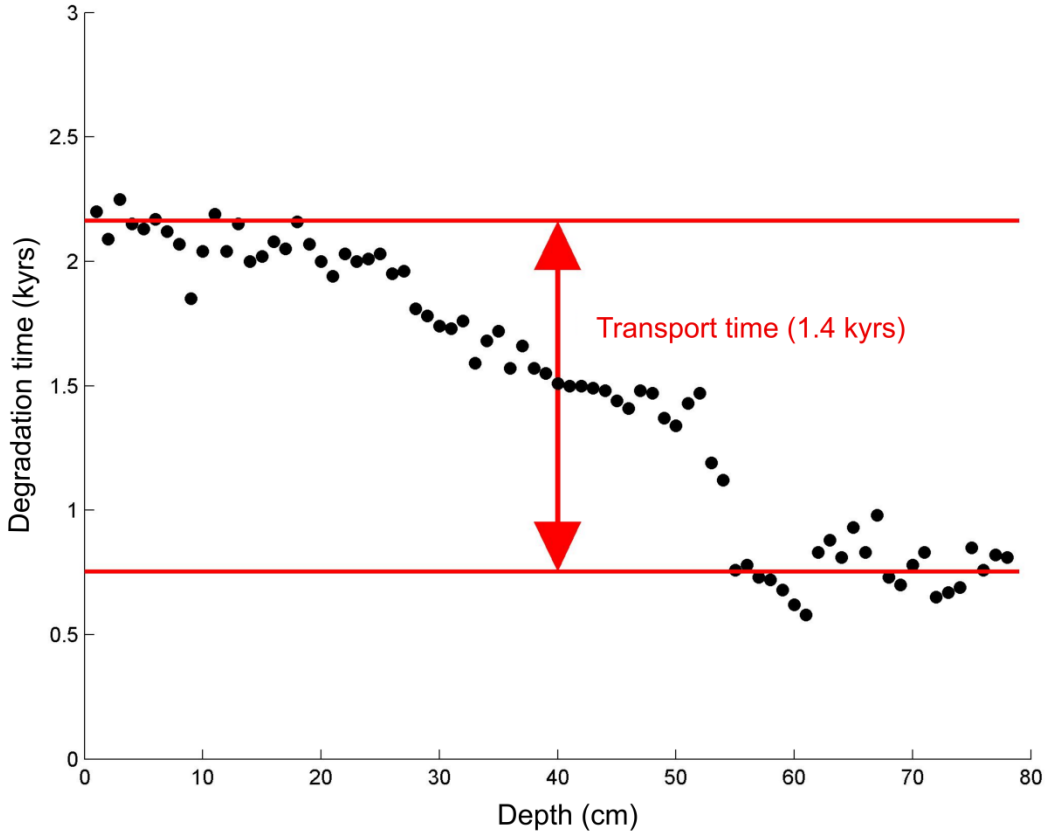

Figure S5. An estimate of the lateral transport time of sediments shown as the degradation time (kyr) against the core depth (cm) in the sediment core GC58. See Supplementary methods for lateral transport time calculations.

Supplementary methods

Source apportionment calculations

In the model for smoothly varying source proportions, data is split into three time-segments of contiguous observations. For each segment, observed $\delta^{13}C$ and $\Delta^{14}C$ are modelled as

$$\delta^{13}C_i = \delta^{13}C^{ICD-PF} \times p_i^{ICD-PF} + \delta^{13}C^{TS-PF} \times p_i^{TS-PF} + \delta^{13}C^{M\ OC} \times p_i^{M\ OC} + \epsilon_i^{13},$$
$$\Delta^{14}C_i = \Delta^{14}C^{ICD-PF} \times p_i^{ICD-PF} + \Delta^{14}C^{TS-PF} \times p_i^{TS-PF} + \Delta^{14}C^{M\ OC} \times p_i^{M\ OC} + \epsilon_i^{14},$$

where ϵ_i^{13} and ϵ_i^{14} are independent zero-mean normally distributed residuals with variances σ_{13}^2 and σ_{14}^2 respectively. Residual variances are assumed equal for the three time-segments. ICD-PF refers to Ice Complex deposit permafrost, TS-PF to topsoil permafrost and M OC to marine organic carbon.

The endmember values $\delta^{13}C^{ICD-PF}$, $\delta^{13}C^{TS-PF}$, $\delta^{13}C^{M\ OC}$, $\delta^{14}C^{ICD-PF}$, $\delta^{14}C^{TS-PF}$ and $\delta^{14}C^{M\ OC}$ are assumed random effects shared within each time-segment and independent between. With the exception of $\delta^{14}C^{ICD-PF}$ they are assumed normally distributed, with means and standard deviations reported earlier. To avoid values below -1000, $\delta^{14}C^{ICD-PF} + 1000$ is instead assumed to be exponentially distributed. Due to different times of deposit, $\delta^{14}C^{ICD-PF}$ means are set to -933, -833 and -800 for the younger, middle and older segment respectively.

In order to account for the time-dependence between proportions, we follow an approach related to that of Parnell et al. (2013) by modelling p_i^{ICD-PF}, p_i^{TS-PF} and $p_i^{M\ OC}$ using Bayesian cubic B-splines after a transformation to the real plane using the additive log-ratio transform,

$$p_i^{ICD-PF} = \frac{\exp(s_1(y_i))}{\exp(s_1(y_i)) + \exp(s_2(y_i)) + 1},$$
$$p_i^{TS-PF} = \frac{\exp(s_2(y_i))}{\exp(s_1(y_i)) + \exp(s_2(y_i)) + 1},$$

and $p_i^{M\ OC} = 1 - p_i^{ICD-PF} - p_i^{TS-PF}$. The functions s_1 and s_2 are the spline-functions and y_i estimated years BP for observation i. Separate/independent splines are used for each of the three time-segments and knots are placed at the centres and endpoints. The model is fitted using rjags (Plummer, 2016) within the R computing environment (R Core Team, 2016). The code for the model is available at https://github.com/mskoldSU/Keskitalo_et_al.

Lateral transport time estimation

The GC58 core spans over a time period of ~ 9,500 cal yrs BP, during which the study area experienced a significant sea level rise (34 m in water depth). This means that the time for lateral transport of the terrestrial organic carbon (terrOC) from the shore to the site of sedimentation increased. To model this transport time the ratio of lignin/terrOC was used as a molecular clock. The fraction remaining lignin/terrOC ($f_{lig/terrOC}$) from remineralisation depends on the degradation of both lignin and terrOC. Bröder et al. (2015) established the following relation for the Laptev Sea (time t in kyrs):

$$f_{lig/terrOC}(t) = \frac{e^{-2.6 \cdot t}}{0.87 \cdot e^{-2.2 \cdot t} + 0.13} \quad (2)$$

The observational concentration terrOC can be established as OC/(1 - f_{marine}), where the fraction marine is derived from the source apportionment results. To obtain the observational $f_{lig/terrOC}$ we need to consider the expected lignin/terrOC signal for the sources that have not been degraded. For ICD-PF the lignin/terrOC ratio is 17.4±8.3 mg g^{-1} and for topsoil-PF 20.9±6.4 mg g^{-1} (Tesi et al., 2016). Since the relative proportions of ICD-PF and topsoil-PF for each data point is known from the source apportionment, the non-degraded lignin/terrOC signatures may be estimated, using Markov chain Monte Carlo (MCMC) techniques to account for the endmember variability. By computing the ratio of the observed and non-degraded lignin/terrOC ratios we can calculate the fraction remaining lignin/terrOC and further, estimate the lateral transport times using Eq. (2).

References

Appleby, P. G. and Oldfield, F.: The calculation of lead-210 dates assuming a constant rate of supply of unsupported ^{210}Pb to the sediment, Catena, 5, 1–8, 1978.

Bröder L., Tesi T., Semiletov I.P., and Gustafsson Ö.: Fate of permafrost-released organic matter in the Laptev Sea: What is its lateral transport time along the transect from the Lena delta area to the deep sea of the Arctic interior?, AGU Fall Meeting, San Francisco, USA, 14–18 December 2015, C33F-06, 2015.

Parnell, A. C., Phillips, D. L., Bearhop, S., Semmens, B. X., Ward, E. J., Moore, J. W., Jackson, A. L. Kelly, D. J and Inger, R.: Bayesian Stable Isotope Mixing Models, , Environmetrics, 24(6), 387–399, doi:10.1002/env.2221, 2013.

Plummer, M.: rjags: Bayesian Graphical Models using MCMC., 2016.

R Core Team: R: A language and environment for statistical computing, 2016.

Tesi, T., Semiletov, I., Hugelius, G., Dudarev, O., Kuhry, P. and Gustafsson, Ö.: Composition and fate of terrigenous organic matter along the Arctic land-ocean continuum in East Siberia: Insights from biomarkers and carbon isotopes, Geochim. Cosmochim. Acta, 133, 235–256, doi:10.1016/j.gca.2014.02.045, 2014.

Tesi, T., Muschitiello, F., Smittenberg, R. H., Jakobsson, M., Vonk, J. E., Hill, P., Andersson, A., Kirchner, N., Noormets, R., Dudarev, O., Semiletov, I. and Gustafsson, Ö.: Massive remobilization of permafrost carbon during post-glacial warming, Nat. Commun., 7, 13653, doi:10.1038/ncomms13653, 2016.